

Room temperature one-step synthesis of microarrays of N-doped flower-like anatase TiO₂
composed of well-defined multilayer nanoflakes by Ti anodization

This article has been downloaded from IOPscience. Please scroll down to see the full text article.

2011 Nanotechnology 22 305607

(<http://iopscience.iop.org/0957-4484/22/30/305607>)

View [the table of contents for this issue](#), or go to the [journal homepage](#) for more

Download details:

IP Address: 59.61.18.30

The article was downloaded on 03/07/2011 at 01:57

Please note that [terms and conditions apply](#).

Room temperature one-step synthesis of microarrays of N-doped flower-like anatase TiO₂ composed of well-defined multilayer nanoflakes by Ti anodization

Chenglin Wang¹, Mengye Wang¹, Kunpeng Xie¹, Qi Wu¹,
Lan Sun¹, Zhiqun Lin² and Changjian Lin^{1,3}

¹ Department of Chemistry, College of Chemistry and Chemical Engineering, Xiamen University, Xiamen 361005, People's Republic of China

² Department of Materials Science and Engineering, Iowa State University, Ames, IA 50011, USA

³ State Key Laboratory of Physical Chemistry of Solid Surfaces, and College of Chemistry and Chemical Engineering, Xiamen University, Xiamen 361005, People's Republic of China

E-mail: sunlan@xmu.edu.cn and cjlin@xmu.edu.cn

Received 4 April 2011, in final form 30 May 2011

Published 1 July 2011

Online at stacks.iop.org/Nano/22/305607

Abstract

Microarrays of N-doped flower-like TiO₂ composed of well-defined multilayer nanoflakes were synthesized at room temperature by electrochemical anodization of Ti in NH₄F aqueous solution. The TiO₂ flowers were of good anatase crystallinity. The effects of anodizing time, applied voltage and NH₄F concentration on the flower-like morphology were systematically examined. It was found that the morphologies of the anodized Ti were related to the anodizing time and NH₄F concentration. The size and density of the TiO₂ flowers could be tuned by changing the applied voltage. The obtained N-doped flower-like TiO₂ microarrays exhibited intense absorption in wavelengths ranging from 320 to 800 nm. Under both UV and visible light irradiation, the photocatalytic activity of the N-doped flower-like TiO₂ microarrays in the oxidation of methyl orange showed a significant increase compared with that of commercial P25 TiO₂ film.

1. Introduction

TiO₂ photocatalysts have attracted considerable attention as highly functional materials due to their semiconductor nature, long term stability, and low-cost preparation for a variety of applications, including the purification of air and water [1, 2], splitting of water into hydrogen [3], and dye-sensitized solar cells [4, 5]. TiO₂ with different morphologies possesses various properties and applications due to its specific size and shape [6]. To this end, the controlled synthesis of TiO₂ with different sizes and shapes has become an increasingly significant topic for material science and technology. Recent research on the synthesis of micro- and nano-materials has shown that these kinds of TiO₂ architectures may promise potential use in catalysts and optoelectronics [7–9].

Anatase TiO₂ exhibits a higher activity than its rutile counterpart because its conduction band is at a higher

energy [1]. Various approaches such as hydrothermal treatment [6, 10], the sol–gel method [11, 12] and calcination processes [13, 14] have been developed to synthesize anatase TiO₂ structures at low temperature, but most of them unavoidably involve the use of either templates or complicated procedures. When anatase TiO₂ is prepared by hydrothermal treatment or sol–gel synthesis, the crystallization usually results in highly reduced properties, structural damage or particle aggregation [15–17]. Similarly, anatase TiO₂ obtained by calcination generally produces large-sized particles, which leads to structural collapse [15]. For a long time, suspensions or compacted nanoparticulate films have mainly been used, based mainly on the commercial Degussa P25 TiO₂ nanopowder.

It is well known that the industrial application of the suspended system in the form of colloidal and particulate TiO₂ in photodegradation of pollutants is seriously limited due

to the difficulty in separating TiO₂ from water or pollutants and recycling the photocatalyst, the particle aggregation especially at high concentration, and the problematic use in continuous flow systems. To overcome these technical problems, various methods have been developed to immobilize TiO₂ films on solid supportive substrates. However, the efficiency of the immobilized systems is much lower than that of the corresponding slurries, because of the inevitable reduction of the overall surface active area associated with the catalyst immobilization. In the past decade, electrochemical anodization has been demonstrated to be a convenient technique for fabricating a variety of TiO₂ films on Ti substrates [18–24]. By tuning the electrochemical parameters, such as the composition and concentration of electrolytes, anodizing voltage, and anodizing time, TiO₂ films with different shapes and sizes can be fabricated [21–24]. However, the as-fabricated TiO₂ films are amorphous [25]. To convert amorphous TiO₂ into anatase phase, thermal annealing at high temperature is necessary [21–24, 26, 27]. Very recently, a few modified approaches were demonstrated to grow partially crystalline, anatase TiO₂ nanotubes at room temperature [28], and totally anatase TiO₂ nanotubes at 60 °C by anodizing Ti substrates [29]. In particular, Grimes *et al* reported a room temperature one-step polyol synthesis of anatase TiO₂ nanotube arrays by an optimized anodization process [30]. In this paper, we report the room temperature one-step synthesis of microarrays of N-doped flower-like anatase TiO₂ composed of well-defined multilayer nanoflakes by a simple electrochemical anodization method. To the best of our knowledge, this is the first study of room temperature synthesis of anatase TiO₂ in an aqueous electrolyte. Notably, this is also the first report on one-step synthesis of N-doped flower-like TiO₂ by Ti anodization. The effects of anodizing time, applied voltage and NH₄F concentration on the morphology of the TiO₂ structures were examined in detail. The light absorption property and photocatalytic activity of the N-doped flower-like anatase TiO₂ microarrays were investigated. The ability to synthesize N-doped anatase TiO₂ materials at room temperature makes them very attractive for practical applications in environmental purification, water photoelectrolysis and solar energy conversion.

2. Experimental details

Titanium foils of 0.1 mm in thickness and a purity of 99.6% were used. Prior to anodization, the Ti foils (1 cm × 1 cm) were ultrasonically cleaned with anhydrous ethanol and distilled water successively, followed by rinsing with DI water and drying in air. The anodization was carried out in a two-electrode electrochemical cell with titanium foil as the working electrode and platinum foil as the counter electrode under constant voltage applied by a direct current (DC) power supply (HY1712-5S, Huaian Yaguang Electronics Co., Ltd). The distance between the working electrode and the counter electrode was 2.5 cm and the electrolyte was an NH₄F aqueous solution. All experiments were carried out at room temperature (~25 °C). After anodization, the samples were immediately rinsed with deionized water, and then dried at

ambient temperature. For comparison, a commercial Degussa P25 TiO₂ powder (a mixture of anatase and rutile) was used to prepare thin particulate film on the Ti foil. P25 film was prepared by dispersing into deionized water first and then depositing on the Ti foil, followed by a heat treatment at 200 °C for 30 min [31]. This procedure was repeated several times until the thickness of the P25 film reached ca. 10 μm.

The structure and morphology of the anodized samples were examined using an LEO-1530 field-emission scanning electron microscope (FESEM) and a Tecnai-F30 high-resolution transmission electron microscope (HRTEM). The crystalline phases of the samples were detected by a Philips X'pert x-ray diffractometer (XRD) with Cu Kα radiation. The composition of the sample was identified by x-ray photoelectron spectroscopy (XPS; VG, Physical Electronics Quantum 2000 Scanning ESCA Microprobe, Al Kα radiation). UV–visible diffuse reflectance spectra of the samples were recorded using a UV–vis–NIR spectrophotometer (Varian Cary 5000).

The photocatalytic activity of the samples was evaluated by the degradation of the methyl orange (MO) azo dye. The photocatalytic experiments were carried out in a quartz glass reactor. The reactor was equipped with a water jacket to control the reaction temperature. A 200 W high-pressure mercury lamp emitting at a wavelength of 365 nm was employed as the UV light source or a 500 W tungsten–halogen lamp ($\lambda \geq 520$ nm) was used to produce the simulated sunlight. All experiments were performed under continuous stirring, using 30 ml of 20 mg l⁻¹ MO aqueous solution, and air was bubbled through the gas disperser into the reactor. The absorbance changes of the MO were monitored using a UV–vis spectrophotometer (Unico UV-2102 PC) at a wavelength of 507 nm.

3. Results and discussion

A representative large-area FESEM image of the TiO₂ microarray synthesized in 0.01 M NH₄F electrolyte at 50 V for 2 h is shown in figure 1(a). A closer examination reveals that vertically oriented bamboo-shoot-like TiO₂ flowers about 2.5–7.0 μm in diameter and 2.1–10.3 μm in height grew on the Ti substrate (figure 1(b)), and the average diameter of the flower bottom and height of the flower are approximately 4.5 μm and 5.2 μm, respectively. Figure 1(c) shows the FESEM image of an individual flower. Further scrutiny of the flowers reveals that the flower-like TiO₂ consists of well-defined layered nanoflakes (figure 1(d); close-up of nanoflower shown in figure 1(c)). The corresponding TEM image shows that the flower-like TiO₂ has a hierarchical structure (figure 1(e)). An HRTEM image of the nanoflake reveals a lattice spacing of 0.352 nm, corresponding to the (101) plane of anatase TiO₂ (figure 1(f)) [32]. The corresponding x-ray diffraction (XRD) pattern is shown in figure 2. The diffraction peaks can be fully indexed to anatase phase TiO₂ (JCPDS 21-1272), indicating that the as-synthesized product was pure anatase TiO₂. The size of TiO₂ crystallites was estimated to be 12 nm from the full-width at half-maximum (FWHM) of the (101) diffraction peak using the Scherrer equation. Some works

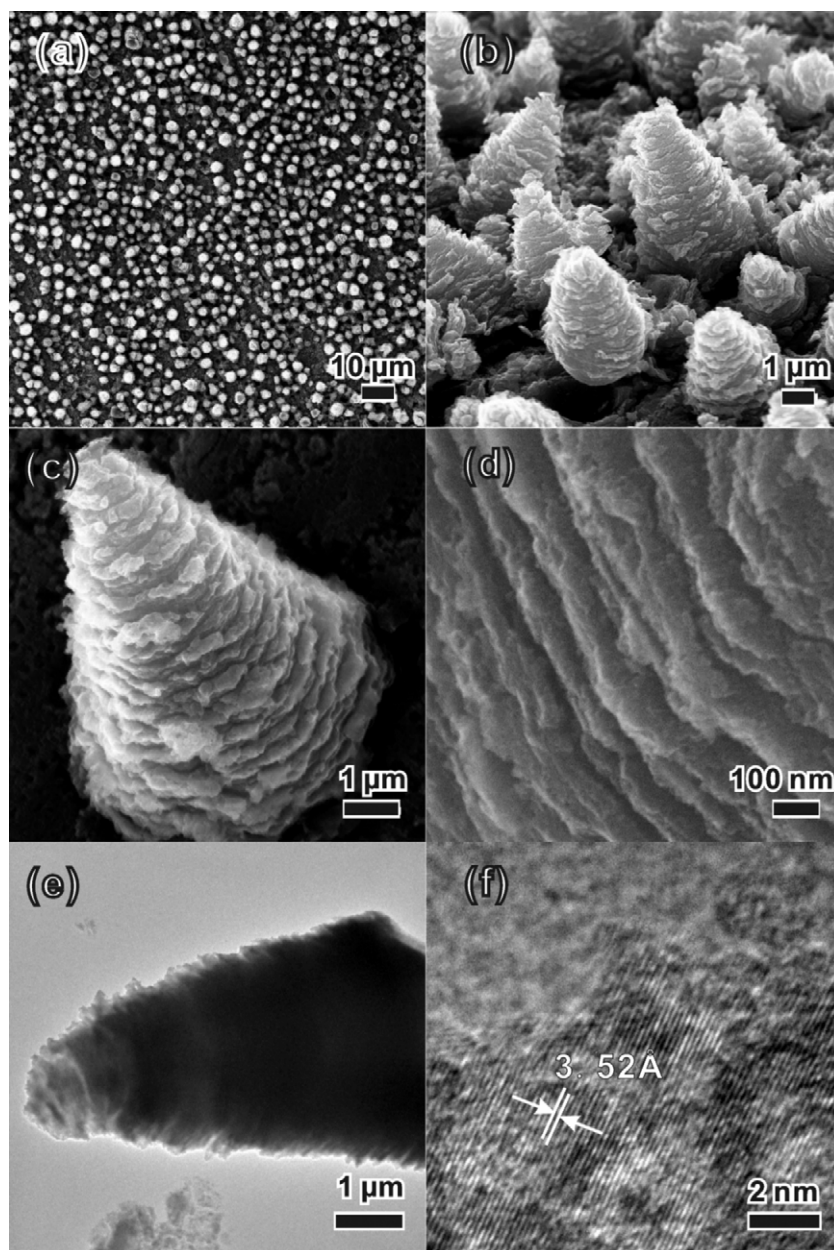


Figure 1. FESEM images of the as-synthesized TiO_2 : (a) a top view, (b) a 3D view, (c) an individual TiO_2 flower, (d) close-up of (c), (e) TEM image and (f) HRTEM image from an individual nanoflake.

have reported the formation of TiO_2 nanotube arrays by the anodization of Ti in various electrolytes containing NH_4F , including 1 M $(\text{NH}_4)_2\text{SO}_4$ [33, 34], 1 M $(\text{NH}_4)_2\text{H}_2\text{PO}_4$ [35], glycerol electrolyte [36] and ‘water-free’ CH_3COOH [37], which respectively contain 0.5 wt% NH_4F . In contrast, a simple aqueous solution containing 0.01 M NH_4F was used in our work; therefore, only flower-like TiO_2 arrays, but not TiO_2 nanotube arrays, were observed in the experiments.

In order to elucidate the formation process of the flower-like TiO_2 microarrays, we investigated the influence of the reaction time when the Ti foils were anodized in the NH_4F solution at a constant anodization potential of 50 V. The FESEM images of the samples yielded at different time periods are shown in figure 3. After 10 min anodization (figure 3(a)),

the surface of the Ti substrate was covered by an initial porous oxide layer [18, 21]. As time increased to 30 min (figure 3(b)), small protrusions appeared randomly on the Ti surface and were considered as the buds of flower-like TiO_2 . As the anodization time progressed to 1 h (figure 3(c)), the protrusions were converted into bamboo-shoot-like TiO_2 (referred to as flower-like TiO_2), and the number of formed flower-like TiO_2 increased. Further increase of the anodization time to 2 h (figure 3(d)) led to increased coverage of the flower-like TiO_2 on the Ti substrate. Finally, the self-organized and vertically oriented flower-like TiO_2 microarray was thus obtained.

Figure 4 shows the current–time response behavior of Ti anodized at 50 V in 0.01 M NH_4F aqueous solution. Such a curve shape, showing a decrease/increase/decrease sequence,

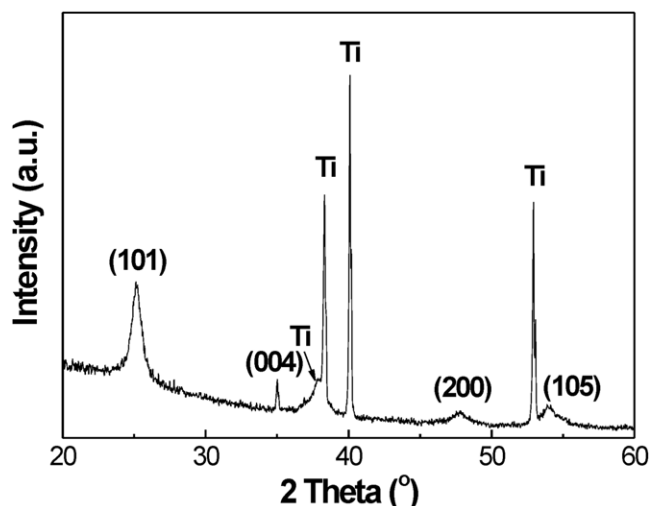


Figure 2. XRD patterns of the as-synthesized TiO₂ microarray.

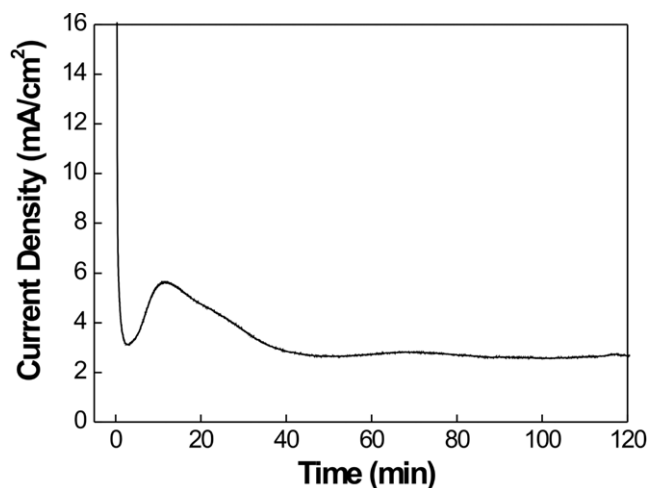


Figure 4. Current density versus time during the anodization of Ti foil in a 0.01 M NH₄F electrolyte at 50 V.

has already been observed for self-organized formation of TiO₂ nanotubes [38, 28]. Initially, the current density dropped sharply due to the formation of a thin oxide layer [39, 40], and then increased to a maximum due to the pitting of the oxide layer which resulted from the field-assisted dissolution [41]. Some quite small TiO₂ grains with defects formed in the preferential sites (marked with arrows in figure 3(a)). Then the current density started to decrease again due to an increase

in the porous depth along with the local dissolution of Ti. The TiO₂ grains tended to coalesce due to the high activity of their respective surface defects [42, 43]. The crystalline transformation temperature for smaller TiO₂ particles is relatively lower [44]. As a consequence, the crystalline TiO₂ nanoflakes formed in the suitable local oxidation environment. In the progress of TiO₂ nanoflake corrosion and precipitation on the surface, crystalline TiO₂ nanoflakes continuously

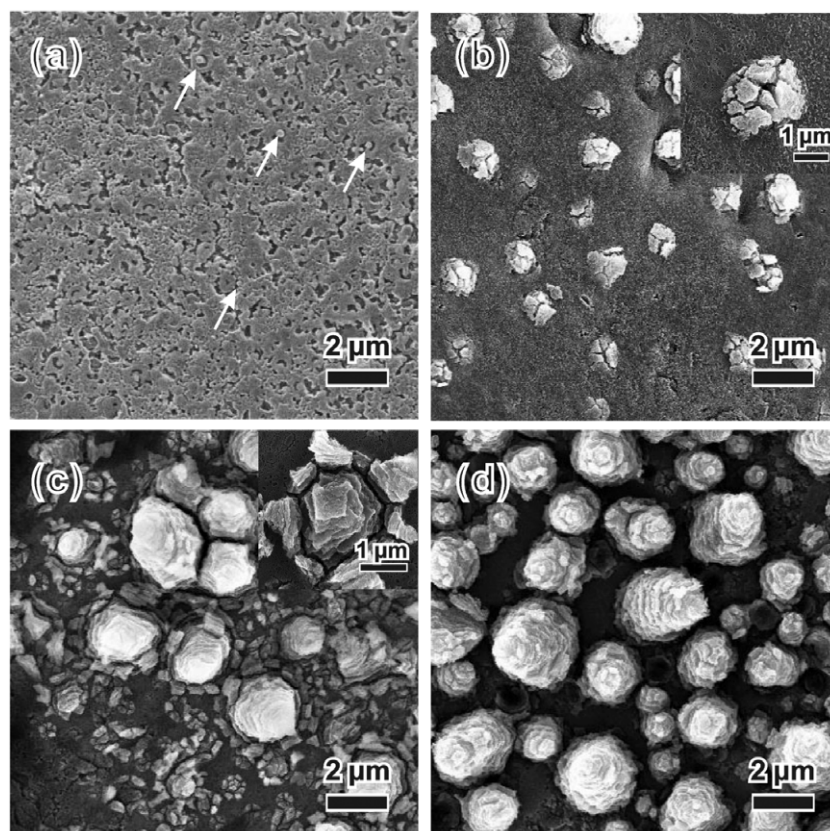


Figure 3. FESEM images showing the evolution of the flower-like structured TiO₂ when the Ti foil was anodized in an NH₄F solution at a constant potential of 50 V for 10 min (a), 30 min (b), 1 h (c) and 2 h (d).

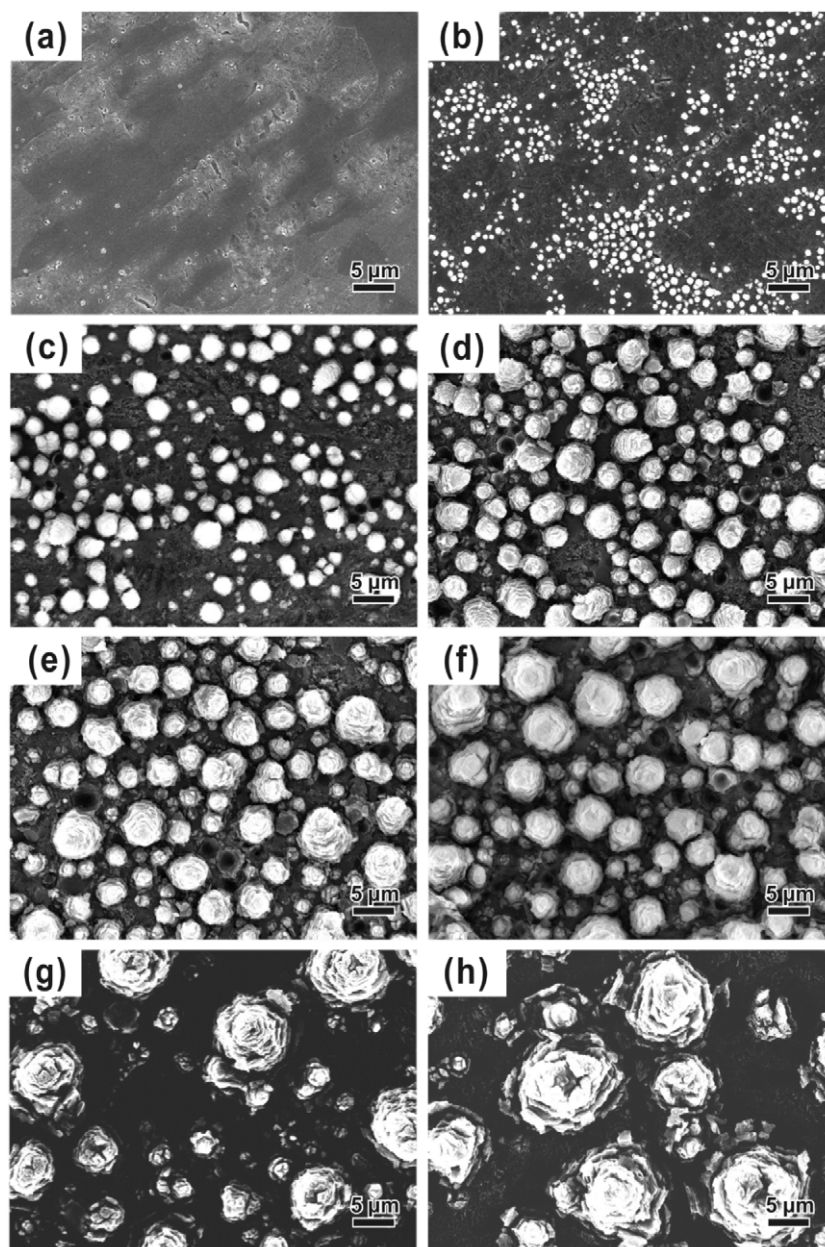


Figure 5. FESEM images of flower-like anatase TiO₂ anodized at different voltages: (a) 20 V, (b) 30 V, (c) 40 V, (d) 50 V, (e) 60 V, (f) 70 V, (g) 80 V, and (h) 90 V.

formed at the bottom of the pores and gradually layered up in the direction normal to the Ti substrate. Some bud-like TiO₂ were shaped by aggregating nanoflakes, which is clearly evident in figure 3(b). As the anodization progressed, flower-like TiO₂ appeared and their size gradually increased with the prolonged anodization time (figure 3(c)). Finally, due to the dynamic balance between the field-assisted oxidation and dissolution as well as the chemical dissolution, the growth of the flower-like TiO₂ was limited to a certain shape and size, and the flower-like anatase TiO₂ with multilayered nanoflakes were thus yielded (figure 3(d)).

In order to assess the influence of other key parameters on the surface morphology, a set of experiments was performed by systematically varying the applied voltages and the NH₄F

concentration. Figures 5(a)–(h) show FESEM images of the flower-like structures obtained at different anodizing voltages (i.e., from 20 to 90 V with a 10 V increment) in 0.01 M NH₄F solution for 2 h. At low anodizing voltage (20 V; figure 5(a)) only a few flower-like particles formed. As the voltage increased from 30 to 50 V (figures 5(b)–(d)), the amount of flower-like particles and their size began to increase. When the applied voltage was at 60 and 70 V (figures 5(e) and (f)), no obvious changes in the size and density of flower-like particles could be observed. As the voltage further increased to above 70 V (figures 5(g) and (h) at 80 V and 90 V, respectively), the size of the flower-like particles continued to increase, while the density decreased. We propose that the formation of the flower-like structures may be related to the low concentration

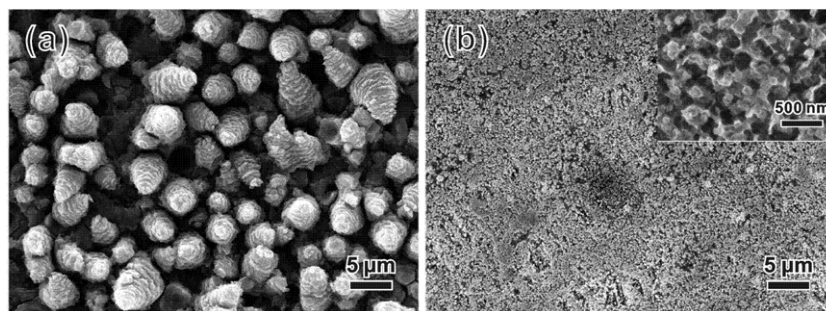


Figure 6. FESEM images of flower-like anatase TiO₂ formed at 50 V for 2 h in 0.05 M NH₄F (a) and 1.0 M NH₄F (b).

of aqueous electrolyte. When the voltage was very low, nearly dense TiO₂ film was obtained which was due to the low etching rate of TiO₂ (mainly electric field induced dissolution); as the voltage increased, flower-like structures started to appear and the structure density decreased with the increase in voltage. As a result, flower-like TiO₂ can be obtained in the range from 30 to 90 V.

Figures 6(a) and (b) represent the FESEM images of the samples formed at 50 V for 2 h in 0.05 M and 1.0 M NH₄F solution, respectively. In the 0.05 M NH₄F solution self-organized flower-like TiO₂ can still be achieved. Anodization in the 1.0 M NH₄F solution, however, resulted in a porous structure. These observations confirmed that there was a chemical equilibrium between the formation and dissolution of TiO₂ during the formation of flower-like TiO₂. When anodization was carried out in low fluorine ion (F⁻) concentration (figure 6(a)), the formation rate of flower-like TiO₂ was faster than the rate of its dissolution, thereby leading to the formation of flower-like morphology. By contrast, when anodization was performed at high F⁻ concentration (figure 6(b)), the dissolution of TiO₂ to form pores occurred according to the reaction [33]



We further studied the light absorption property of the flower-like anatase TiO₂ microarray. For comparison, P25, one of the best commercial TiO₂ photocatalysts, was chosen as the benchmark. Figure 7 shows a comparison of UV-vis diffuse reflectance spectra for the flower-like anatase TiO₂ microarray anodized in 0.01 M NH₄F electrolyte at 50 V for 2 h in which the TiO₂ flowers show relatively uniform size and larger density and a P25 film whose thickness was the same as the largest height of the TiO₂ flowers (approximately 10 μm). A significant absorption of P25 film at wavelength shorter than 400 nm can be assigned to the intrinsic band gap absorption of anatase phase TiO₂ (≈3.2 eV). By contrast, the flower-like anatase TiO₂ microarray exhibited a much stronger absorption in the range from 320 to 800 nm and a remarkable red shift in the band gap transition. A previous report showed that TiO₂ nanotube arrays prepared by the anodization of Ti in an electrolyte without NH₄F, such as HF aqueous solution, did not exhibit visible light absorption [45]. However, in our experiment, the flower-like anatase TiO₂ microarray prepared by the anodization of Ti in NH₄F aqueous solution without any

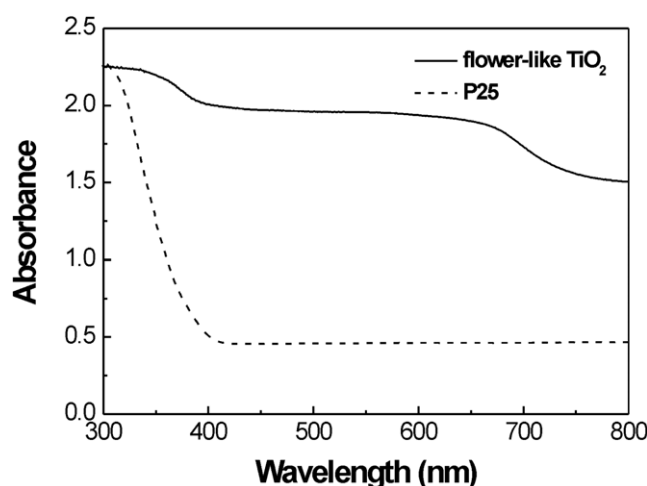


Figure 7. UV-vis diffuse reflectance spectra of the N-doped flower-like anatase TiO₂ and the P25 film.

organic compound exhibited stronger visible light absorption, indicating that the presence of NH₄⁺ in the electrolyte plays a key role in the visible light absorption. The intense visible light response of the flower-like anatase TiO₂ microarray could be primarily attributed to the doping of N in the TiO₂. In addition, the unique flower-like morphology of anatase TiO₂ and its hierarchical structures composed of layered nanoflakes could lead to more reflectance of the light.

The form of the N in the flower-like anatase TiO₂ was determined by XPS. The XPS spectrum (figure 8(a)) indicated that the as-prepared flower-like anatase TiO₂ contained Ti, O, N, F and a trace amount of C. The atomic ratio of Ti:O was 1:2.25, which is much larger than stoichiometric TiO₂. To identify the chemical state of O, Ar⁺ sputtering was performed to remove a 5 nm surface layer. After Ar⁺ sputtering, the atomic ratio of Ti:O was 1:2.0, indicating that the excess oxygen at the surface of the flower-like TiO₂ should be attributed to surface adsorbed oxygen. The existence of the C element can be ascribed to the adventitious hydrocarbon from the XPS instrument itself. In order to uncover the origin of the N and F signals, high-resolution XPS spectra of the N 1s region and the F 1s region of the sample anodized in 0.01 M NH₄F electrolyte at 50 V for 2 h were performed and are shown in figures 8(b) and (c), respectively. A broad peak in the range from 396 to 404 eV (figure 8(b)), with a maximum

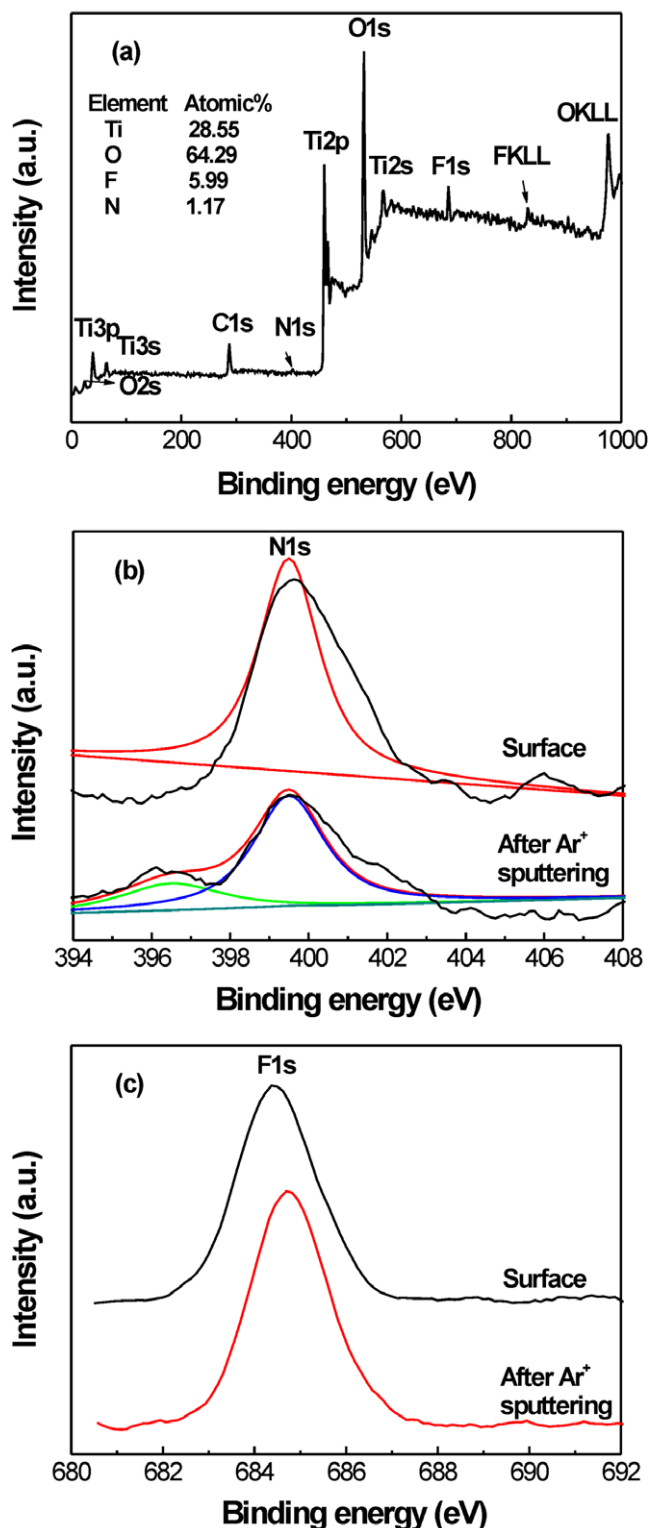


Figure 8. XPS spectra of (a) the flower-like TiO₂ over a large energy range, (b) N 1s and (c) F 1s.

(This figure is in colour only in the electronic version)

located at the binding energy of 399.6 eV, was clearly evident, which can be attributed to N 1s [46, 47]. A similar peak at nearly 399.6 eV was also identified in other literature [48, 49] from the ammonia-treated TiO₂ and could be assigned to the

N 1s band of interstitial doped N atoms [50, 51]. After Ar⁺ sputtering, this peak became a little weak. It is noteworthy that a weak peak at 396–397 eV was detected and attributed to the N 1s band of substitutional nitrogen atoms that can be identified with the atomic β-N states [43]. Therefore, N from the NH₄F solution was doped into the TiO₂ crystal lattice. As shown in figure 8(c), the peak located at 684.4 eV can be attributed to the F⁻ ions physically adsorbed on the surface of the TiO₂ [8, 34, 52]. After Ar⁺ sputtering, this peak became a little weak and no new peak appeared, indicating that the F⁻ ions in the electrolyte were only physically adsorbed on the surface of TiO₂. Accordingly, the significant visible light absorption of the flower-like anatase TiO₂ mainly resulted from the doping of N in TiO₂. In this context, it may be expected that the as-synthesized flower-like anatase TiO₂ microarrays may display an outstanding visible light photocatalytic activity.

To this end, the photocatalytic activity of the N-doped flower-like anatase TiO₂ microarray was examined using methyl orange (MO) as a probe molecule. We tested the photocatalytic activity of four kinds of TiO₂ microarrays anodized in 0.01 M NH₄F aqueous solution at 40, 50, 60, and 70 V for 2 h. It was found that the sample anodized in 0.01 M NH₄F electrolyte at 50 V for 2 h exhibited the highest photocatalytic activity. Figures 9(a) and (b) show the photodegradation curves of MO in the presence of the N-doped flower-like anatase TiO₂ microarray which exhibited the highest photocatalytic activity and P25 film under UV and visible light irradiation, respectively. The linear relationship of $\ln(c/c_0)$ versus time (figures 9(c) and (d)) shows that the photocatalytic degradation of MO followed a pseudo-first-order expression [53]:

$$\ln(C_0/C) = kt \quad (2)$$

where k is the apparent first-order rate constant (min^{-1}), C_0 and C are the initial and reaction concentrations of MO dye, respectively. Under UV irradiation (figure 9(c)), the apparent rate constant for the N–F-doped flower-like anatase TiO₂ was 0.0544 min^{-1} , which was about two times larger than that of the P25 film, 0.0268 min^{-1} . The unique morphology and hierarchical structure of flower-like anatase TiO₂ may play an important role in enhancing the UV photocatalytic activity of TiO₂. The hierarchical structure composed of nanoflakes allowed an effective light-scattering inside the gaps between nanoflakes, resulting in the photogenerated electrons and holes to participating effectively in the photocatalytic degradation of contaminants [46]. Moreover, the micro–nano architecture of flower-like anatase TiO₂ shortened the path of photogenerated charge transfer at the interface [54]. Under visible light irradiation (figure 9(d)), the apparent rate constant for the N-doped flower-like anatase TiO₂ was 0.00476 min^{-1} , which was more than three times larger than that of the P25 film, 0.00156 min^{-1} , further confirming that the flower-like anatase TiO₂ exhibited excellent visible light photocatalytic activity for promising environmental applications. To check the potential reusability and stability of the N–F-doped flower-like anatase TiO₂ photocatalyst in the reaction medium, we performed a series of five photocatalytic cycles using the N-doped flower-like anatase TiO₂ microarray anodized in 0.01 M NH₄F

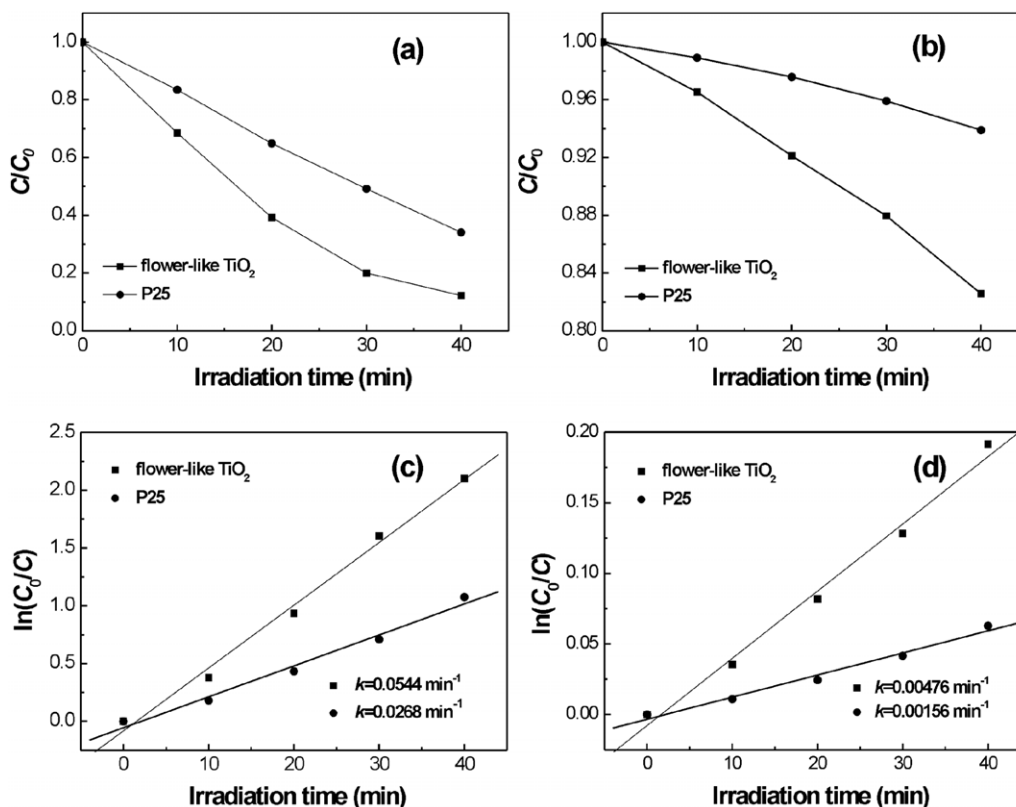


Figure 9. Photodegradation curves of MO assisted by the N-doped flower-like anatase TiO₂ and the P25 film under UV (a) and visible light (b) irradiation. The fitting results using the pseudo-first-order reaction under UV and visible light irradiation are shown in (c) and (d), respectively.

electrolyte at 50 V for 2 h. The MO photodegradation as well as the first-order reaction constant k did not vary significantly, and the results were reproducible within 5%, indicating that the photocatalyst can be safely reused. In the present study, the N-doped flower-like anatase TiO₂ microarray was synthesized by anodizing Ti foil in NH₄F aqueous solution at room temperature and exhibited excellent visible light photocatalytic activity. As a result, no thermal annealing is necessary and the resulting N-F-doped flower-like anatase TiO₂ microarrays can be readily used for practical applications.

4. Conclusion

In summary, we reported the room temperature one-step synthesis of microarrays of N-doped flower-like anatase TiO₂ composed of well-defined multilayer nanoflakes by a simple, low-cost electrochemical anodization method. The applied voltage and the concentration of NH₄F electrolyte played a crucial role in the growth of the flower-like anatase TiO₂ microarrays on the Ti substrate. The resulting N-doped flower-like anatase TiO₂ microarrays exhibited strong visible light response and excellent photocatalytic activity in the degradation of organic pollutants. The N-doped flower-like anatase TiO₂ material synthesized in the present study was directly grown on the Ti substrate at room temperature, dispensing with high temperature thermal annealing, thereby giving it great potential in environmental purification, water photoelectrolysis, and solar energy utilization.

Acknowledgments

This work was supported by the National Natural Science Foundation of China (21021002 and 51072170) and NFFTBS (J1030415).

References

- [1] Linsebigler L A, Lu G and Yates J T 1995 *Chem. Rev.* **95** 735
- [2] Wang R, Hashimoto K, Fujishima A, Chikuni M, Kojima E, Kitamura A, Shimohigoshi M and Watanabe T 1997 *Nature* **388** 431
- [3] Fujishima A and Honda K 1972 *Nature* **238** 37
- [4] Ngamsinlapasathian S, Sakulkhaemaruethai S, Pavasupree S, Kitiyanan A, Sreethawong S, Suzuki Y and Yoshikawa S 2004 *J. Photochem. Photobiol. A* **164** 145
- [5] Onoda K, Ngamsinlapasathian S, Fujieda T and Yoshikawa S 2007 *Sol. Energy Mater. Sol. Cells* **91** 1176
- [6] Wang F M, Shi Z S, Gong F, Jiu J T and Adachi M 2007 *Chin. J. Chem. Eng.* **15** 754
- [7] Huang J Q, Huang Z, Guo W, Wang M L, Cao Y G and Hong M C 2008 *Cryst. Growth Des.* **8** 2444
- [8] Wu G S, Wang J P, Thomas D F and Chen A C 2008 *Langmuir* **24** 3503
- [9] Wu J M and Qi B 2007 *J. Phys. Chem. C* **111** 666
- [10] Jitputti J, Rattanaavoravipa T, Chuangchote S, Pavasupree S, Suzuki Y and Yoshikawa S 2009 *Catal. Commun.* **10** 378
- [11] Uekawa N, Kajiwara J, Kakegawa K and Sasaki Y 2002 *J. Colloid Interface Sci.* **250** 285
- [12] Zhou L and O'Brien P 2008 *Phys. Status Solidi A* **205** 2317

- [13] Mor G K, Varghese K, Paulose O M, Shankar K and Grimes C A 2006 *Sol. Energy Mater. Sol. Cells* **90** 2011
- [14] Macak J M, Tsuchiya H, Ghicov A, Yasuda K, Hahn R, Bauer S and Schmuki P 2007 *Curr. Opin. Solid State Mater. Sci.* **11** 3
- [15] Serrano D P, Calleja G, Sanz R and Pizarro P 2007 *J. Mater. Chem.* **17** 1178
- [16] Li Y, White T J and Lim S H 2004 *J. Solid State Chem.* **177** 1372
- [17] Allam N K, Shankar K and Grimes C A 2008 *Adv. Mater.* **20** 3942
- [18] Zwilling V, Aucouturier M and Darque-Ceretti E 1999 *Electrochim. Acta* **45** 921
- [19] Gong D W, Grimes C A, Varghese O K, Hu W C, Singh R S, Chen Z and Dickey D C 2001 *J. Mater. Res.* **16** 3331
- [20] Hahn R, Macak J M and Schmuki P 2007 *Electrochem. Commun.* **9** 947
- [21] Wang J and Lin Z Q 2008 *Chem. Mater.* **20** 1257
- [22] Wang J and Lin Z Q 2009 *J. Phys. Chem. C* **113** 4026
- [23] Wang J, Zhao L, Lin V S Y and Lin Z Q 2009 *J. Mater. Chem.* **19** 3682
- [24] Wang J and Lin Z Q 2010 *Chem. Mater.* **22** 579
- [25] Macak J M and Schmuki P 2006 *Electrochim. Acta* **52** 1258
- [26] Ruan C M, Paulose M, Varghese O K, Mor G K and Grimes C A 2005 *J. Phys. Chem. B* **109** 15754
- [27] Habazaki H, Shimizu K, Nagata S, Skeldon P, Thompson G E and Wood G C 2002 *Corros. Sci.* **44** 1047
- [28] Yoriya S, Mor G K, Sharma S and Grimes C A 2008 *J. Mater. Chem.* **18** 3332
- [29] Xiao X F, Ouyang K G, Liu R F and Liang J H 2008 *Appl. Surf. Sci.* **255** 3659
- [30] Allam N K and Grimes C A 2009 *Langmuir* **25** 7234
- [31] Macak J M, Zlamal M, Krysa J and Schmuki P 2007 *Small* **3** 300
- [32] Wu J M, Zhang T W, Zeng Y W, Hayakawa S, Tsuru K and Osaka A 2005 *Langmuir* **21** 6995
- [33] Macak J M, Tsuchiya H and Schmuki P 2005 *Angew. Chem. Int. Edn* **44** 2100
- [34] Taveira L V, Macák J M, Tsuchiy H, Dick L F P and Schmuki P 2005 *J. Electrochem. Soc.* **152** B402
- [35] Ghicov A, Tsuchiya H, Macák J M and Schmuki P 2005 *Electrochem. Commun.* **7** 505
- [36] Macak J M, Tsuchiya H, Taveira L, Aldabergerova S and Schmuki P 2005 *Angew. Chem. Int. Edn* **44** 7463
- [37] Tsuchiya H, Macák J M, Taveira L, Balaur E, Ghicov A, Sirotna K and Schmuki P 2005 *Electrochem. Commun.* **7** 576
- [38] Tengvall P, Elwing H and Lundström I 1989 *J. Colloid Interface Sci.* **130** 405
- [39] Zhang H Z and Banfield J F 1999 *Am. Mineral.* **84** 528
- [40] Zhang J, Xu Q, Li M, Feng Z and Li C 2009 *J. Phys. Chem. C* **113** 1698
- [41] Macak J M, Hildebrand H, Marten-Jahns U and Schmuki P 2008 *J. Electroanal. Chem.* **621** 254
- [42] Pan J H, Zhang X, Du A J, Sun D D and Leckie J O 2008 *J. Am. Chem. Soc.* **130** 11256
- [43] Asahi R, Morikawa T, Ohwaki T, Aoki K and Taga Y 2001 *Science* **293** 269
- [44] Chen X and Burda C 2004 *J. Phys. Chem. B* **108** 15446
- [45] Lai Y K, Sun L, Chen Y C, Zhang H F, Lin C J and Chen J W 2006 *J. Electrochem. Soc.* **153** D123
- [46] Li H X, Li J X and Huo Y N 2006 *J. Phys. Chem. B* **110** 1559
- [47] Sathishi M, Viswanathan B, Viswanath R P and Gopinath C S 2005 *Chem. Mater.* **17** 6349
- [48] Diwald O, Thompson T L, Goralski E G, Walck S D and Yates J T 2004 *J. Phys. Chem. B* **108** 6004
- [49] Gao B F, Ma Y, Cao Y A, Yang W S and Yao J N 2006 *J. Phys. Chem. B* **110** 14391
- [50] Di Valentin C, Pacchioni G, Selloni A, Livraghi S and Giamello E 2005 *J. Phys. Chem. B* **109** 11414
- [51] Livraghi S, Paganini M C, Giamello E, Selloni A, Di Valentin C and Pacchioni G 2006 *J. Am. Chem. Soc.* **128** 15666
- [52] Zhou J K, Lv L, Yu J Q, Li H L, Guo P Z, Sun H and Zhao X S 2008 *J. Phys. Chem. C* **112** 5316
- [53] Qu J H and Zhao X 2008 *Environ. Sci. Technol.* **42** 4934
- [54] Kontos A I, Arabatzis I M, Tsoukleris D S, Kontos A G, Bernard M C, Petrakis D E and Falaras P 2005 *Catal. Today* **101** 275